Accepted Manuscript

Synthesis, Biological Evaluation, and Physicochemical Property Assessment of 4-Substituted 2-phenylaminoquinazolines as Mer Tyrosine Kinase Inhibitors

Sheng-Biao Wang, Mutian Cui, Xiao-Feng Wang, Emika Ohkoshi, Mostar Goto, De-Xuan Yang, Linna Li, Shoujun Yuan, Susan L. Morris-Natschke, Kuo-Hsiung Lee, Lan Xie
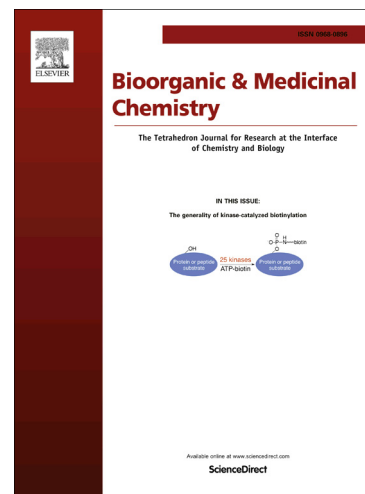
Please cite this article as: Wang, S-B., Cui, M., Wang, X-F., Ohkoshi, E., Goto, M., Yang, D-X., Li, L., Yuan, S., Morris-Natschke, S.L., Lee, K-H., Xie, L., Synthesis, Biological Evaluation, and Physicochemical Property Assessment of 4-Substituted 2-phenylaminoquinazolines as Mer Tyrosine Kinase Inhibitors, *Bioorganic & Medicinal Chemistry* (2016), doi: http://dx.doi.org/10.1016/j.bmc.2016.05.025

Synthesis, Biological Evaluation, and Physicochemical Property Assessment of 4-Substituted 2-phenylaminoquinazolines as Mer Tyrosine Kinase Inhibitors

Sheng-Biao Wang,[a] Mutian Cui,[a] Xiao-Feng Wang,[a,d] Emika Ohkoshi,[b] Mostar Goto,[b] De-Xuan Yang,[c] Linna Li,[c] Shoujun Yuan,[c] Susan L. Morris-Natschke,[b] Kuo-Hsiung Lee,[b,e,*] Lan Xie [a,b,*]

[a] *Beijing Institute of Pharmacology & Toxicology, 27 Tai-Ping Road, Beijing, 100850, China*

[b] *Natural Products Research Laboratories, UNC Eshelman School of Pharmacy, University of North Carolina at Chapel Hill, NC 27599, USA*

[c] *Beijing Institute of Radiation Medicine, 27 Tai-Ping Road, Beijing, 100850, China*

[d] *Pharmacy Department, Urumqi General Hospital, Lanzhou Military Region, Urumqi, 830000, China*

[e] *Chinese Medicine Research and Development Center, China Medical University & Hospital, Taichung, Taiwan*

*Corresponding authors. E-mail: lanxie4@gmail.com; Tel/Fax: 86-10-66931690 (L. Xie); E-mail: khlee@unc.edu; Tel: 919-962-0066; Fax: 919-966-3893 (K.H. Lee)

Abstract

Current results identified 4-substituted 2-phenylaminoquinazoline compounds as novel Mer tyrosine kinase (Mer TK) inhibitors with a new scaffold. Twenty-one 2,4-disubstituted quinazolines (series **4–7**) were designed, synthesized, and evaluated against Mer TK and a panel of human tumor cell lines aimed at exploring new Mer TK inhibitors as novel potential antitumor agents. A new lead, **4b**, was discovered with a good balance between high potency (IC_{50} 0.68 μM) in the Mer TK assay and antiproliferative activity against MV4-11 (GI_{50} 8.54 μM), as well as other human tumor cell lines (GI_{50} < 20 μM), and a desirable druglike property profile with low log P value (2.54) and high aqueous solubility (95.6 μg/mL). Molecular modeling elucidated an expected binding mode of **4b** with Mer TK and necessary interactions between them, thus supporting the hypothesis that Mer TK might be a biologic target of this kind of new active compound.

Graphic Abstract

4b
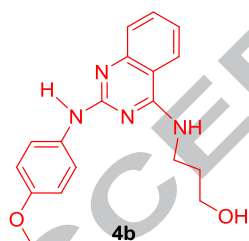
IC_{50} 0.68 μM (Mer kinase)
GI_{50} 8.54 μM in MV4-11 cells
aq. solubility 95.6 μg/mL
log P 2.54 (pH 7.4)
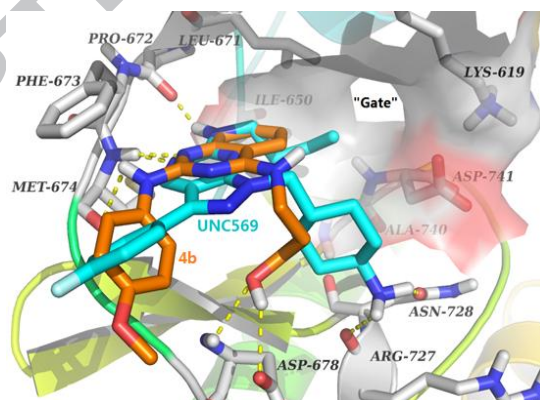
Abbreviations:

ALL, acute lymphocytic leukaemia; ADMET, absorption, distribution, metabolism, elimination and toxicity; A549, human lung cancer cell line; DU145, prostate cancer cell line; GI_{50}, effective concentration for 50% cell growth inhibition; HTCL, human tumor cell lines; IC_{50}, effective concentration that inhibits 50% Mer tyrosine kinase; K562, human chronic myelogenous leukemia cell line; KB, nasopharyngeal carcinoma cell line; KB-vin, vincritstine-resistant KB subline cell line; Mer TK, Mer tyrosine kinase; MV4-11, acute leukemia cell line; PDB, protein data base; SAR, structure-activity relationship.

Introduction

Mer tyrosine kinase (Mer TK) is a member of the TAM (Tyro3/Axl/Mer) kinase family and has been identified as a specific therapeutic target for acute lymphoblastic leukemia (ALL), [1] the most common malignant cancer in children. Despite a significant improvement in ALL treatment in terms of survival (>80%) over the past 40 years,[2] novel targeted therapies for pediatric ALL are urgently needed, because current standard therapy treatments induce short- and long-term toxicities,[3,4] plus development of resistance and relapse. The Mer TK plays a critical role in the pathogenesis of ALL through initiation of anti-apoptotic signaling via increased phosphorylation of Akt and Erk, and subsequent prevention of cell apoptosis,[5] and is ectopically expressed at high-levels in pediatric T- and B-cell acute lymphoblastic leukemias in vitro and in vivo in contrast to normal lymphocytes.[6] The overexpression of Mer TK in T- and B-cells has provided compelling evidence that inhibition of Mer reduces the survival of leukemic cells, makes cells more susceptible to death, and significantly delays the onset of disease in a xenograft mouse model of leukemia.[7] Additionally, over- or ectopic-expression of Mer TK is also associated with a wide spectrum of human cancers and other diseases, including thrombosis, autoimmune disease, and retinitis pigmentosa.[8] Therefore, the Mer receptor tyrosine kinase is a very promising selective therapeutic target for new anticancer drugs, not only for pediatric ALL, but possibly for other leukemias and adult solid tumors.[9] As a new biological target, the crystal structure of Mer TK was first identified by a complex with C-52, a weak Mer inhibitor.[10] Subsequently, small molecular Mer kinase inhibitors, including UNC569,[11] UNC2250,[12] and UNC2881[13] (Figure 1), with subnanomolar inhibitory potency were discovered and crystal structures of Mer TK complexed with these new ligands have also reported. These results should greatly assist the exploration of novel Mer tyrosine kinase inhibitors for treatment of ALL and other cancers.
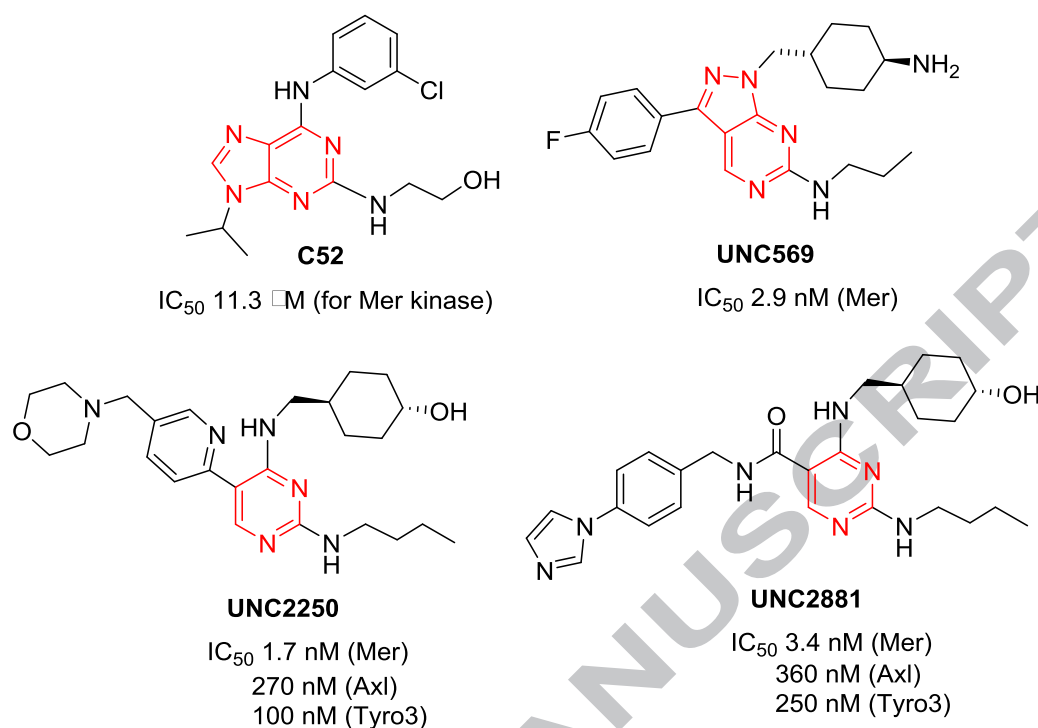
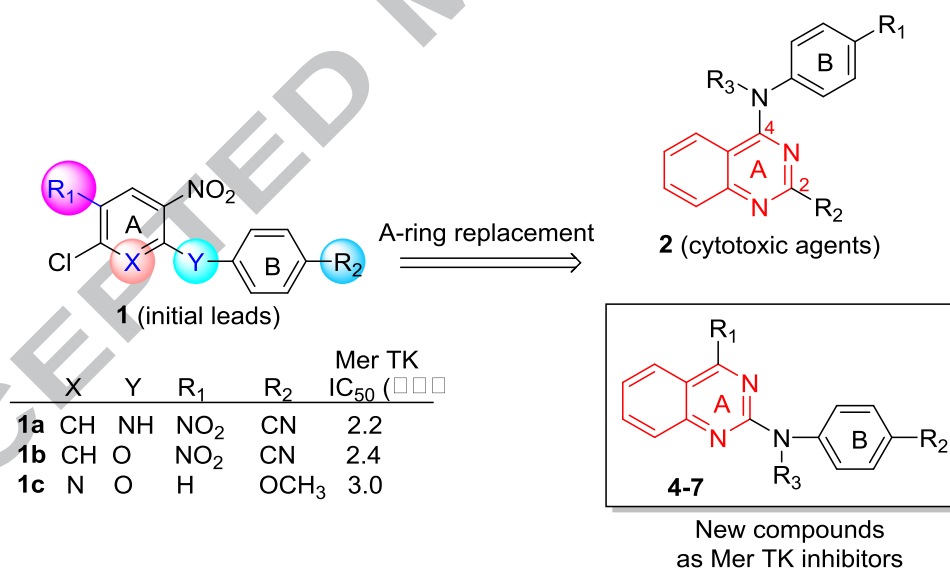**Figure 1** The Mer TK inhibitors reported

**Figure 2** Initial leads, modification strategy, and new compounds designed

In our prior study, high throughput screening of 72 kinases led to the initial discovery of Mer TK inhibitors leads **1a-c** with simple and similar scaffolds (Figure 2). 5-Chloro-*N*-4-cyanophenyl-

2,4-dinitro aniline (**1a**) and two analogues **1b** and **1c** showed selective inhibition against Mer tyrosine kinase (IC_{50} 2.2–3.0 μM) without activity against Tyro3 and Axl kinases (IC_{50} > 30 μM) in the TAM (Tyro3/Axl/Mer) kinase family.[14] Meanwhile, the three compounds also clearly exhibited anticancer activity with low micromolar GI_{50} values ranging from 0.33 to 4.79 μM in a human tumor cell line (HTCL) panel, including A549 (human lung cancer), KB (nasopharyngeal carcinoma), KB-vin (vincristine- resistant KB subline), DU145 (prostate cancer), and K562 (human chronic myelogenous leukemia cells). With this starting point, some structural optimizations were conducted to explore novel Mer kinase inhibitors with a new scaffold as anticancer agents. Based on a structure analysis of several known Mer TK inhibitors as shown in Figure 1, we observed that the pyrimidine ring is a common structural core moiety and appropriate substituents are positioned in a binding orientation at the Mer TK binding site. To increase the probability of generating successful advanced leads, the phenyl or pyridine ring (A-ring) of the initial leads **1a-c** was replaced with other bioisosteric aromatic rings in our following lead modifications. After several attempts, the quinazoline ring system was found to be a better structural core moiety, leading to a series of 2-substituted 4-phenylamino-quinazoline compounds **2** (Figure 2) with extremely high antitumor potency (GI_{50} < 10 nM) in several cellular assays as well as in vivo.[15,16,17] However, the series **2** compounds did not show inhibitory activity in Mer TK assays (IC_{50} >30 μM); thus, their antitumor target is not the Mer TK. However, when the phenylamino moiety (B-ring) was positioned at the 2-position of the quinazoline ring (A ring), the resulting 2-phenylaminoquinazoline compounds exhibited obvious inhibitory potency against Mer TK with low micromolar IC_{50} values. Therefore, several series of 4-substituted 2-phenylaminoquinazoline compounds (**4–7** series) were designed, synthesized, and evaluated in Mer tyrosine kinase and human tumor cell line (HTCL) assays aimed at exploring the new type of Mer TK inhibitor leads. As shown in Figure 2, our structural modifications were focused on the three substituents, R^1 at the 4-position on the quinazoline
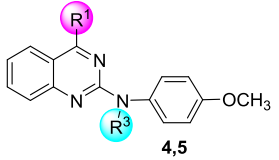
ring (A-ring), R^2 on the phenyl ring (B-ring), and R^3 on the nitrogen (N) linker between the A- and B-rings, while a phenyl ring was maintained at the 2-position of the quinazoline. Herein, we reported new series of 4-substituted 2-arylaminoquinazolines **4–7**, including synthesis, biological activity in Mer TK and cellular assays, assessment of essential physicochemical properties associated with ADMET profiles, and structure-acitivity relationship (SAR) discussion as well as molecular modeling demonstrated at targeting Mer tyrosine kinase.

Chemistry

A facilitated synthetic route to target compounds **4–7** is illustrated in Scheme 1. Commercially available 2,4-dichloroquinazoline was coupled with various amines at room temperature in THF for 1 h to preferentially produce 4-alkylamino-2-chloroquinazolines **3a-f** in 60-95% yields, due to the higher reactivity of the 4-chloro compared with the 2-chloro position on the quinazoline ring.[18] Next, 4-methoxy-*N*-substituted-anilines were reacted with the 2-chloro on quinazolines **3b-f** in the presence of a stronger base *t*-BuOK and catalyst Pd(OAc)$_2$/X-phos in a mixed solvent of *t*-BuOH and toluene under microwave irritation at 130 ºC to obtain the corresponding 4-alkylamino-2-(4-methoxyphenyl)amino quinazolines **4b-f**, respectively, in 33–54% yields. Alternatively, *N*-methyl-4-methoxyaniline or other *para*-substituted anilines were coupled with **3a-f** in EtOH under microwave irritation at 150 ºC to yield target compounds **5a-e**, **4a**, **6a-e**, and **7a-f**, respectively. All target compounds were identified by NMR and MS data.
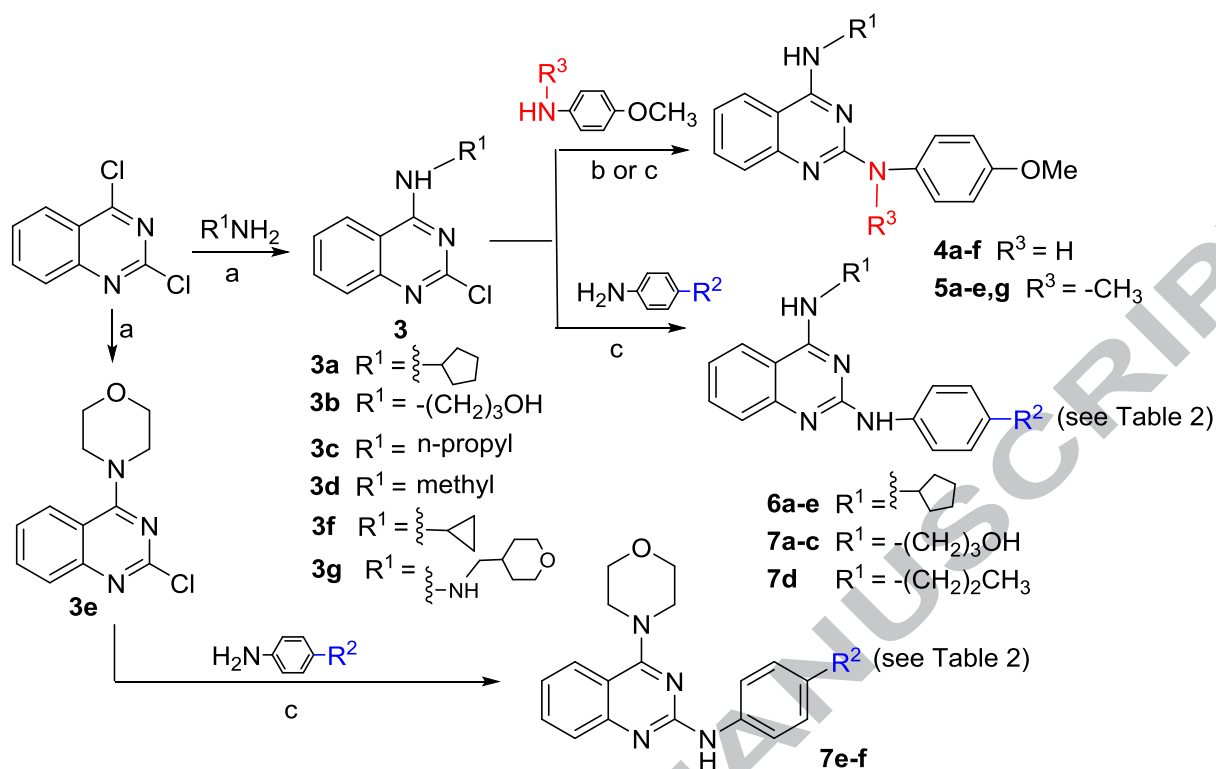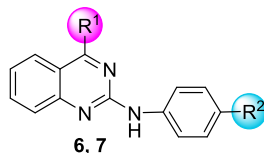
Scheme 1. (a) THF, rt, < 60 min; (b) *t*-BuOK (2 equiv.), Pd(OAc)$_2$/X-phos (5% and 4% equiv.), *t*-BuOH/toluene (v:v 0.5/2.5 mL), microwave, 130 ºC, 15 min (for **4b-f**); (c) EtOH, microwave, 150 ºC, 15−25 min.

Table 1 Biological activities and physicochemical properties of series **4** and **5**

	R^1	R^3	$IC_{50}(\mu M)^a$ Mer TK	$GI_{50}(\mu M)^b$					Properties^c	
				A549	KB	KB-vin	DU145	MV4-11	Aq. Sol. (μg/mL)	Log P
4a	–NH–cyclopentyl	H	1.08	10.1	11.1	12.6	12.4	4.91	10.4	>5
5a	–NH–cyclopentyl	Me	1.14	9.4	11.7	10.1	10.2	2.70	1.11	>5
4b	N–propanol(OH)	H	0.68	15.2	20.3	17.1	18.3	8.75	95.6	2.54
5b	N–propanol(OH)	Me	2.01	13.0	24.8	30.8	30.2	70.1	ND	ND
4c	–NH–propyl	H	3.43	3.53	5.33	5.09	4.08	5.88	4.36	>5
5c	–NH–propyl	Me	1.84	12.4	13.7	12.4	13.0	2.33^e	3.43	>5
4d	–NH–	H	2.25	16.1	14.8	17.5	14.3	3.07	6.61	3.21
5d	–NH–	Me	10.2	19.9	18.7	22.9	24.3	ND	ND	ND
4e	morpholine	H	2.06	20.1	21.0	15.3	20.1	ND	ND	ND
5e	morpholine	Me	>30	ND^d	ND	ND	ND	ND	ND	ND
4f	–NH–cyclopropyl	H	3.56	13.0	13.3	13.4	13.0	<13.4	ND	ND
5g	NH–CH2–tetrahydropyran	Me	>30	ND	ND	ND	ND	ND	ND	ND
Staurosporine^f			0.083							
Paclitaxel (nM)^f				4.9	2.6	948	2.6	ND		

^{a} The concentration that inhibits 50% Mer tyrosine kinase; ^{b} The concentration inhibits 50% human tumor cell growth, averaged values determined by at least three independent experiments; ^{c} active compounds with IC_{50} <10 μM and GI_{50} <20 μM were measured by the methods in Reference 19; ^{d} not detected; ^{e} tested in human chronic myelogenous leukemia (K526) cells; ^{f} reference compounds as the passitive control in related assays.

Table 2 Biological activities and physicochemical properties of series **6** and **7**

	R^1	R^2	IC_{50} (μM) [a] Mer TK	GI_{50} (μM) [b]					Property [c]	
				A549	KB	KB-vin	DU145	MV4-11	Aq. Sol. (μg/mL)	Log P
4a	–NH–cyclopentyl	OMe	1.08	10.1	11.1	12.6	12.4	4.91	10.4	>5
6a	–NH–cyclopentyl	CN	>30	>31.3	>31.3	>31.3	>31.3	ND [d]	ND	ND
6b	–NH–cyclopentyl	NH_2	7.27	15.9	17.4	21.7	18.7	4.42	ND	ND
6c	–NH–cyclopentyl	F	4.17	12.8	13.8	12.3	9.9	5.43	1.54	>5
6d	–NH–cyclopentyl	OH	1.24	14.8	12.1	13.6	14.3	3.00	3.10	3.95
6e	–NH–cyclopentyl	COOH	2.90	28.7	25.2	19.8	27.3	7.50	ND	ND
4b	NH–CH₂CH₂CH₂–OH	OMe	0.68	15.2	20.3	17.1	18.3	8.75	95.6	2.54
7a	NH–CH₂CH₂CH₂–OH	CN	1.72	3.00	23.7	4.31	18.7	2.79	7.52	2.84
7b	NH–CH₂CH₂CH₂–OH	NH_2	>30	17.1	19.7	18.7	20.8	ND	ND	ND
7c	NH–CH₂CH₂CH₂–OH	F	>30	19.3	17.1	24.2	20.6	ND	ND	ND
7d	–NH–ethyl	F	7.84	4.3	2.9	2.5	4.2	ND	ND	ND
7e	–N(morpholine)	F	>30	ND	ND	ND	ND	ND	ND	ND
7f	–N(morpholine)	NH_2	>30	ND	ND	ND	ND	ND	ND	ND
Staurosporine [e]			0.083							
Paclitaxel (nM) [e]				4.9	2.6	948	2.6			

[a] IC_{50} is concentration that inhibits 50% Mer tyrosine kinase; GI_{50} is concentration that inhibits 50% human tumor cell growth, and the values were averaged values determined by at least three independent experiments; [c] *active* compounds with IC_{50} <10 μM and GI_{50} <20 μM were measured by the methods in Reference 19; [d] not detected; [e] reference compounds as the passitive control in related assays.

Results and discussion

All 4-substituted 2-phenylaminoquinazoline compounds (series **4–7**) were first evaluated for inhibition of Mer TK in a high throughput screening platform with staurosporine as a positive control.[11] The first two series of 4-substituted 2-(*para*-methoxyphenyl)aminoquinazolines **4** (R^3 = H) and **5** (R^3 = Me) were designed to investigate effects of various alkyl groups (R^1) at the 4-position of the quinazoline, and their biological data are shown in Table 1. Except **5e** and **5f** (>30 μM), most series **4** and **5** compounds exhibited obvious inhibitory activity in the Mer TK assay with low micromolar IC_{50} values of 0.68 to 10.2 μM. These results indicated that the 2-phenylaminoquinazoline is likely a fundamental pharmacophore of this new class of Mer-TK inhibitors. However, comparatively, series **4** compounds were generally as or more potent than corresponding series **5** compounds in the same assay (see **4a** vs **5a**, **4b** vs **5b**, **4d** vs **5d**, and **4e** vs **5e**), suggesting that the methyl substituent (R^3) on the *N*-linker between the two aryl rings (A and B rings) was not essential for enhanced inhibitory activity against Mer TK. However, the 4-substituent (R^1) on the quinazoline ring was modifiable based on the activity shown with a variety of 4-alkylamino groups (R^1) from linear chains of different lengths (**b–d**) or small rings from three- to six-membered (**f, a, e, g**). The 4-(3-hydroxypropyl)amino linear chain (R^1 = $NH(CH_2)_3OH$) resulted in the most potent compound **4b** with an IC_{50} value of 0.68 μM in the Mer TK assay, but the presence of a six-membered ring in the R^1 substituent (**5e** and **5g**) led to decreased or abolished potency. Subsequently, the impact of the substituent (R^2) at the *para*-position of the phenyl B-ring on biological activity was explored by series **6** and **7**, in which R^3 on the N-linker is hydrogen (H). Series **6**, with the same R^1 substituent (4-cyclopentylamino) found in **4a**, contained various *para*-R^2 substituents. Compared with **4a** (R^2 = OMe, IC_{50} 1.08 M), **6d** with a *para*-hydroxy (R^2 = OH) substituent showed a similar low IC_{50} value of 1.24 M. Three other series **6** compounds [**6b** (R^2 = NH_2), **6c** (R^2 = F) and **6e** (R^2 = COOH)] displayed IC_{50} values from 2.96 to 7.27 M, three- to seven-fold less potent than **4a**,

whereas **6a** (R^2 = CN) was inactive (IC_{50} >30 M) in the Mer TK assay. Three of the series **7** compounds (**7a–7c**) contain the same linear chain R^1 group (4-NH(CH$_2$)$_3$OH) found in **4b**. Although less potent than **4b**, compound **7a** (R^2 = CN) still exhibited significant potency (IC_{50} = 1.72 μM), especially, as compared with inactive **6a**. Meanwhile, **7b** (R^2 = NH$_2$) and **7c** (R^2 = F) were inactive (IC_{50} >30 μM), in contrast to the corresponding **6b** and **6c** in the same assay. Moreover, **7d** (R^1 = 4-propylamino, R^2 = F) was less potent (IC_{50} = 7.84 M) than the corresponding **4c** and **5c** (R^1 = 4-propylamino, R^2 = OMe, R^3 = H or Me). Consistent with the results of **5e** and **5g**, compounds **7e** and **7f** with a morpholine in the R^1 position were inactive (IC_{50} >30 M) in the Mer TK assay. Altogether, the current results indicated that both R^1 and R^2 substituents could affect the potency against Mer TK, even though clear relationships were not always observed. These results demonstrated that a *para*-methoxy group (R^2 = OMe) on the phenyl B-ring was generally more favorable than several other R^2 substituents (particularly, COOH, NH$_2$, F) for Mer TK inhibitory potency. Regardless, a R^2 group with strong electronegativity (e.g., F) or electron-withdrawing effect (COOH, CN), as either H-bond acceptor or donor, might interfere with the interactions between the small molecule and Mer TK.

Subsequently, compounds (series **4–7**) active in Mer TK assay, except **5e**, **5g**, **7e**, and **7f** (IC_{50} > 30 μM), were further evaluated in cellular assays against a human tumor cell line (HTCL) panel, including A549, KB, KB-vin, and DU145 cell lines, to determine their antiproliferative activity. Paclitaxel was used as the positive reference. As shown in Tables 1 and 2, most of the new compounds exhibited moderate potency with GI_{50} values less than 20 μM. Notably, similar potencies were generally observed against both KB and drug-resistant KB-vin cell lines, indicating that these compounds are not substrates of Pgp, a membrane efflux-pump protein. Among them, **4c** and **7d** showed the highest overall antiproliferative potency (GI_{50} 3.53–5.09 M and 2.5–4.3 M respectively). Interestingly, compound **7a** (R^1 = -NH(CH$_2$)$_3$OH, R^2 = CN) showed selective potency against A549 (GI_{50} 3.00 M) and

12

drug-resistant KB-vin (GI$_{50}$ 4.31 M) cell growth, five- to eight-fold more potent than against DU145 (GI$_{50}$ 18.7 M) and KB cell lines (GI$_{50}$ 23.7 M). This result suggested that the R^2-group on the B-ring might affect the selectivity in different cell lines. With the criteria of IC$_{50}$ < 10 μM and GI$_{50}$ < 30 μM in the above cellular assays, 13 active compounds were chosen and further tested against the MV4-11 (acute leukemia) cell line, because the Mer kinase is especially overexpressed in T- and B-cell acute lymphoblastic leukemia cells. Except **5b**, most of the tested compounds exhibited low micromolar GI$_{50}$ values against this cell line, with two- to four-fold higher potency than against the prior four tested cell lines. The high potency and selectivity in MV4-11 cells are supportive for this compound type as new antitumor agents targeting Mer TK.
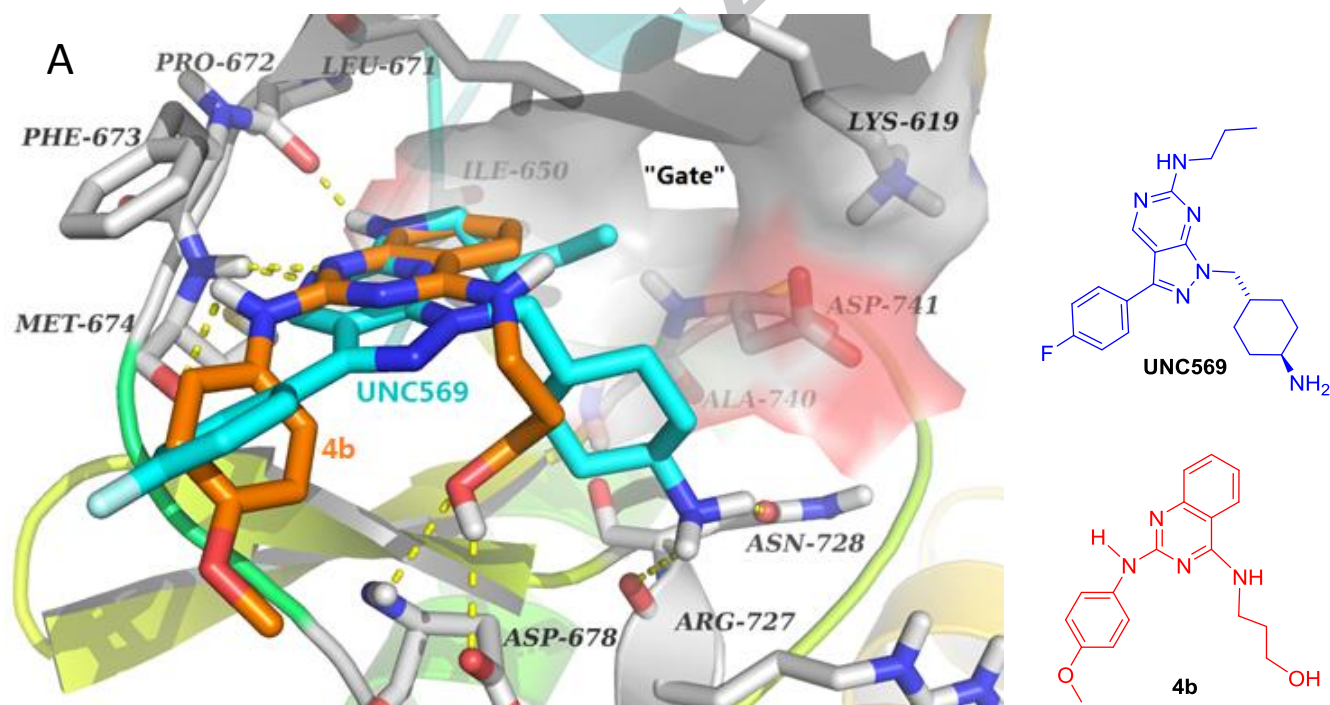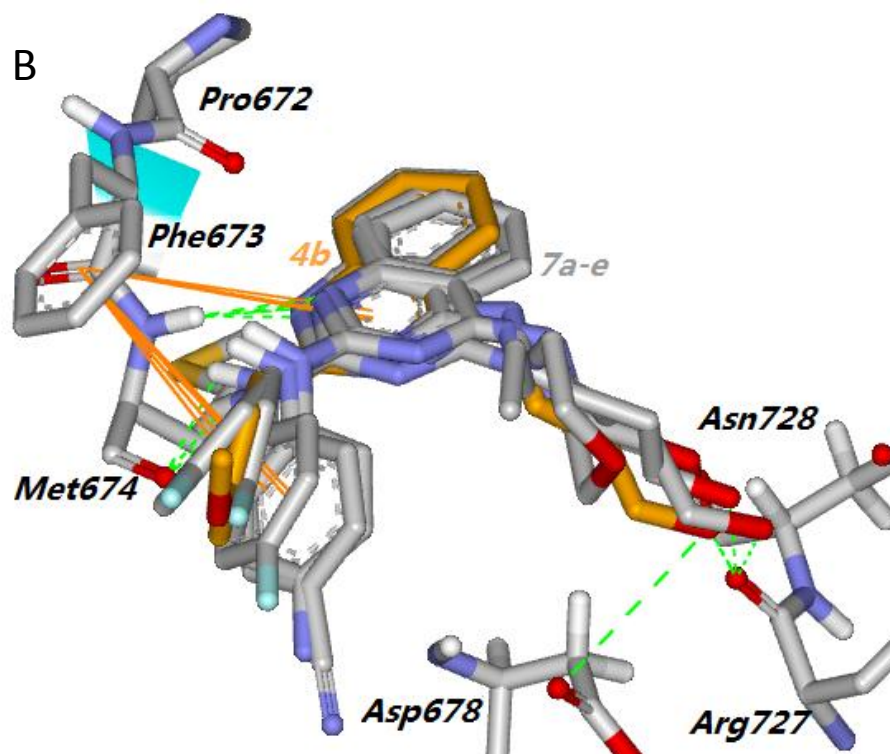
Figure 3 (A) Predicted binding mode of **4b** (orange) with Mer kinase (PDB code: 3TCP) overlapped with UNC569 (cyan, the original bound ligand of 3TCP). Surrounding amino acid side chains are shown in gray stick format and are labeled. Surface is added on the amino acids Lys619, Leu671, Ile650, Ala740 and Asp741 to show the forming "gate". Hydrogen bonds are shown by yellow dashed lines, and the distance between ligands and protein is less than 3 Å. Oxyen atoms are red and nitrogen atoms are blue in ligands and amino acid residues. (B) The binding modes of compounds **7a-7e** (gray) superimposed on **4b** (orange).

To demonstrate that Mer TK could be a target of the active new compounds, we performed molecular modeling studies with Discovery Studio 3.0 (Accelrys) docking into the ligand-specificity active site of Mer TK mapped by several co-crystal structures of Mer with ligands.[10] The crystal structure of Mer kinase in complex with ligand UNC569 (PDB code: 3TCP)[11] from the RCSB Protein Data Bank (http://www.rcsb. org/pdb) was used to dock the most active compound **4b** and predict a

potential binding mode for 4-alkylamino-2-arylaminoquinazolines. As shown in Figure 3A, the pyrazolopyrimidine ring of original ligand UNC569 (cyan stick) was located near the "gate" of the protein and sustained the orientation and overall binding conformation of its substituents at the Mer TK binding site. Original ligand UNC569 showed four hydrogen bonds with Mer kinase: two within the hinge region produced by the nitrogen on the pyrimidine ring with the NH of residue Met674 as well as the NH of the propylamino side chain with the carbonyl of residue Pro672, and two additional hydrogen bonds from the primary amino group on the methylcyclohexyl moiety with the carbonyls of Arg727 and Asn728, respectively. As expected, representative compound **4b** displayed a predicted binding model with Mer TK similar to that of UNC569 as shown in Figure 3. Compound **4b** (orange stick) superimposed well with UNC569, having a similar binding orientation and four hydrogen bonds with the Mer kinase site. Two H-bonds were formed between the key amino acid Met674 with the nitrogen on the quinazoline ring and the NH linker of **4b**, respectively, supporting the conclusion that a NH linker is favorable for higher potency compared with a methylated N-linker (comparison of series **4** and **5**). Two additional H-bonds were produced between the OH in the 4-substituent (R^1) of **4b** with the backbone carbonyl and amino groups, respectively, of Asp678. In addition, a π-π interaction was observed between the phenyl ring of Phe673 and the quinazoline rings in **4b**, which also superimposed over the pyrazolopyrimidine rings of UNC569. The calculated binding free energy of **4b** was -18.25 kcal/mol. Therefore, the docking results of **4b** supported the possibility that compounds of this new type could act as Mer tyrosine kinase inhibitors. Furthermore, compounds **7a-7e**, either active or inactive against Mer TK, were also docked to the Mer TK binding site in the same manner and superimposed with **4b** (in orange). As shown in Figure 3B, **7a-7e** (in gray) have the same binding orientation as that of **4b** and similar interactions around key amino acids Phe673, Met674, and Arg727 (or Asn728). Notably, the π-π interaction between the phenyl ring (B-ring) at the 2-position of the quinazoline with Phe673 was also

observed in this series of compounds, thus demonstrating that the 2-phenylamino moiety is a necessary pharmacophore for Mer TK inibition. Meanwhile, different binding conformations of the B-ring moiety in this compound series are also observed in Figure 3B. Thus, molecular potency related with the B-ring conformations could be affected by flexibility of the NH-linker and different para-substituents (R^2) on the B-ring.

To increase drug discovery success, the druglike properties of active compounds mtust also be considered as a prominent component, in addition to potency, during the early stages of lead optimization. Consequently, nine promising compounds, based on the Mer TK (IC_{50} <5 M) and MV4-11 cellular (GI_{50} <10 M) assay results, were further assessed for essential instrinsic physicochemical properties of aqueous solubility and lipophilicity that are associated with ADME drug properties, potency, and adverse safety. Aqueous solubility and log P values were measured by HPLC methods[19] at pH 7.4, similar to the physiological condition in plasma, and the data are listed in Tables 1 and 2. The experimental log P values of **4b**, **4d**, **6d**, and **7a** fell within a desirable range of 2.54 3.95 (<4) and the remaining compounds **4a**, **5a**, **4c**, **5c**, and **6c** possessed higher lipophilicity (log P > 5). Notably, **4b**, the most potent compound against Mer TK (IC_{50} 0.68 µM), displayed a desirable log P value of 2.54 and relatively high solubility of 95.6 µg/mL, signifying a good balance that should contribute favorably to better ADME profiles. With the same R^1 substituent as **4b**, compound **7a** also showed a low log P value (2.84) and moderate aqueous solubility (7.52 µg/mL), suggesting that the polar 4-(3-hydroxy)propylamino substituent (R^1) in **4b** and **7a** led to lower molecular lipophilicity. Concomitant with increased molecular lipophilicity, **4d** (log P 3.21) and **6d** (log P 3.95) displayed decreased aqueous solubilities of 6.61 µg/mL and 3.10 µg/mL, respectively. Based on data comparison of **4a** vs **5a** and **4c** vs **5c** in Table 1, the presence of a methyl group (R^3) might lead to a decrease in the molecular aqueous solubility. On the other hand, the aqueous solubility results for **4a** (R^2 = OMe), **6c**

(R^2 = F), and **6d** (R^2 = OH) revealed the following favorable order: OMe > OH > F.

Conclusion

In the current study, twenty-one 4-substituted 2-phenylaminoquinazolines (series **4–7**) were designed, synthesized, and evaluated against Mer TK and a human tumor cell line panel. Among them, 13 compounds showed high inhibitory potency against Mer TK with low micromolar IC_{50} values ranging from 0.68 to 4.17 μM. Most of these promising compounds also exhibited significant antiproliferative activity against the MV4-11 cell line (IC_{50} < 10 μM), as well as a broad HTCL panel with moderate IC_{50} values (< 20 μM). Further assessment of physicochemical properties in vitro identified three new lead compounds **4a**, **4b**, and **7a** with a favorable balance between potency in Mer TK and cellular assays and druglike properties of aqueous solubility and lipophilicity. In particular, compound **4b** had an IC_{50} of 0.68 μM against Mer TK, moderate GI_{50} values ranging from 8 to 20 μM in cellular assays, a desirable log P value of 2.54, and high aqueous solubility (95.6 μg/mL). Molecular modeling studies predicted a reasonable binding mode of **4b** with Mer TK similar to that of the known Mer kinase inhibitor UNC569, supporting our hypothesis that Mer TK might be a biologic target of **4b**. Current results demonstrated that (1) the phenylamino moiety at the 2-position on the quinazoline ring (A-ring) is necessary for inhibitory potency against Mer TK; (2) the R^1 at the 4-position on the quinazoline ring is modifiable and its H-bonds formed with Asp678, Arg 727, or Asn278 on the binding site of Mer TK are critical to enhance potency in both Mer TK and cellular assays as well as improve drug-like properties; (3) the *para*-R^2 on the phenyl B-ring greatly affects molecular potency, and a methoxy group (OMe) is better than other groups such as OH, NH$_2$, COOH, F; (4) the NH linker between two aryl rings is favorable to enhance molecular potency compared with the methyl group (R^3) on the N-linker that might benefit the balance between molcular lipophilicity and aqueous solubility. Therefore, the current studies discovered a series of new Mer TK inhibitors with a 4-substituted

2-phenylaminoquinazoline scaffold and provided helpful directions for further lead optimization aimed at the discovery and development of highly potent and selective Mer inhibitors as novel anticancer agents.

Experimental Section

Chemistry. Melting points were measured on a SGW X-4 Micro-Melting point detector without correction. The proton nuclear magnetic resonance (^{1}H NMR) spectra were measured on a JNM-ECA-400 (400 MHz) spectrometer using tetramethylsilane (TMS) as internal standard. The solvent used was DMSO unless indicated. Mass spectra (MS) were measured on an API-150EX mass spectrometer with electrospray ionization connected with an Agilent 1100 system. The microwave reactions were performed on a microwave reactor from Biotage, Inc. Thin-layer chromatography (TLC) was performed on silica gel GF254 plates. Silica gel GF254 and H (200–300 mesh) from Qingdao Haiyang Chemical Company was used for TLC and preparative TLC, respectively. Medium-pressure column chromatography was performed using a CombiFlash companion system from ISCO, Inc. to purify target compounds. All chemicals were obtained from Beijing Chemical Works or Sigma-Aldrich, Inc. The purity of target compounds was measured with HPLC methods and reached >95% for biological assays. The HPLC analyses were performed by using an Agilent 1200 HPLC system with a UV detector and an Agilent Eclipse XDB-C18 column (150 mm × 4.6 mm, 5 μm) under the conditions of elution with 35-70% acetonitrile (CAN)) in water, flow rate 0.8 mL/min, UV detection at 254 nm, and injection volume of 15 L.

General preparation of 2-chloro-4-(*N*-substituted)aminoquinazolines 3a-f. A mixture of 2,4-dichloroquinazoline (1.0 equiv) and an amine (2.0 equiv) in THF (ca. 10 mL) was stirred at room temperature for 0.5–3 h monitored by TLC until the reaction finished. After solvent was removed under reduced pressure, solid crude product was washed with water, dried, and purified by flash column

chromatography (gradient eluention: EtOAc/petroleum ether, 0–50%) to give corresponding compounds **3a-f** in yields of 60–95%. The structures of intermediame **3a** and **3b** as representive compounds were identified with MS and ^{1}H NMR spectra as indicated below.

2-Chloro-4-(*N*-cyclopentyl)aminoquinazoline (3a). Starting with 2,4-dichloro quinazoline (2 g, 10 mmol) and cyclopentanamine (1.7 g, 20 mmol) to produce 2.3 g of **3a** in 93 % yield, white solid, mp 108~110 °C; ^{1}H NMR δ ppm 1.61 (4H, m, CH$_2$×2), 1.75 (2H, m, CH$_2$), 2.03 (2H, m, CH$_2$), 4.50 (1H, f, J = 7.2 Hz, CH), 7.53 (1H, td, J = 8.4 and 1.2 Hz, H-6), 7.60 (1H, d, J = 8.4 Hz, ArH-5), 7.79 (1H, td, J = 8.4 and 1.2 Hz, ArH-7), 8.37 (1H, d, J = 8.4 Hz, ArH-8), 8.46 (1H, d, J = 7.2 Hz, NH); MS *m/z* (%) 248 (M + 1, 20), 250 (M + 3, 8), 144 (100).

2-Chloro-4-((3-hydroxypropyl)amino)quinazoline (3b). Starting with 2,4-dichloro quinazoline (2 g, 10 mmol) and 3-aminopropan-1-ol (1.5 g, 20 mmol) to produce 2.2 g of **3b** in 92 % yield, white solid, mp 93~95 °C; ^{1}H NMR δ ppm 1.81 (2H, f, J = 7.2 Hz, CH$_2$), 3.52 and 3.57 (each 2H, m, CH$_2$), 4.58 (1H, t, J = 4.8 Hz, OH,), 7.53 (1H, t, J = 8.0 Hz, H-6), 7.61 (1H, d, J = 8.0 Hz, ArH-5), 7.79 (1H, t, J = 8.0 Hz, ArH-7), 8.26 (1H, d, J = 8.0 Hz, ArH-8), 8.73 (1H, br, NH); MS *m/z* (%) 238 (M + 1, 40), 240 (M + 3, 13), 144 (100).

General procedure for synthesis of 4b-f. A mixture of a 4-substituted 2-chloroquinazoline (**3b-f**) (1.0 equiv) and 4-methoxyaniline (1.05-1.5 equiv) in the presence of *t*-BuOK (2 equiv), X-Phos (0.04 equiv), Pd(OAc)$_2$ (0.05 equiv), and Celite (300 mg) in *t*-BuOH (0.5 mL) and toluene (2.5 mL) was heated at 130 C for 15 min under microwave irradiation in a closed vial. EtOAc (5 mL) was then added to the mixture, precipitated solid was filtered off, and solvent was removed from the filtrate under reduced pressure to obtain crude products. Purification by flash column chromatography (gradient methanol/DCM ether, 0–5%) provided corresponding pure target compounds.

4-(3-Hydroxypropyl)amino-2-(4-methoxyphenyl)aminoquinazoline (4b). Starting with

2-chloro- 4-(3-hydroxypropyl)aminoquinazoline (**3b**) (105 mg, 0.44 mmol) and 4-methoxyaniline (65 mg, 0.52 mmol) to produce 48 mg of **4b** in 34% yield, white solid, mp 114~116 ℃; ^{1}H NMR (CDCl$_3$) δ ppm 1.88 (2H, f, J = 5.6 Hz, CH$_2$), 3.73 (2H, t, J = 5.6 Hz, NCH$_2$), 3.79 (2H, t, J = 5.6 Hz, OCH$_2$) 3.80 (3H, s, OCH$_3$), 6.23 (1H, br, OH), 6.88 (2H, d, J = 8.8 Hz, ArH-3′, 5′), 7.14 (1H, td, J = 8.0, ArH-6), 7.53~7.58 (3H, m, ArH-5, 7, 8), 7.59 (2H, d, J = 8.8 Hz, ArH-2′, 6′); MS m/z (%) 325 (M + 1, 100).

2-(4-Methoxyphenyl)amino-4-propylaminoquinazoline (4c). Starting with 2-chloro-4-(N-propylamino)quinazoline (**3c**) (270 mg, 1.22 mmol) and 4-methoxyaniline (225 mg, 1.83 mmol) to produce 204 mg of **4c** in 54% yield, yellow solid, mp 220~222 ℃; ^{1}H NMR δ ppm 0.92 (3H, t, J = 7.2 Hz, CH$_3$), 1.66 (2H, six, J = 7.2 Hz, CH$_2$), 3.49 (2H, m, CH$_2$,), 3.78 (3H, s, OCH$_3$), 7.01 (2H, d, J = 8.8 Hz, ArH-3′, 5′), 7.44 (1H, t, J = 8.4 Hz, ArH-6), 7.48 (2H, d, J = 8.8 Hz, ArH-2′, 6′), 7.56 (1H, d, J = 8.4 Hz, ArH-5), 7.81(1H, t, J = 8.4 Hz, ArH-7), 8.38 (1H, d, J = 8.4 Hz, ArH-8), 9.85 (1H, br, NH), 10.32 (1H, s, NH); MS m/z (%) 309 (M + 1, 100).

2-(4-Methoxyphenyl)amino-4-methylaminoquinazoline (4d). Starting with 2-chloro-4-(N-metnyl) aminoquinazoline (**3d**) (150 mg, 0.78 mmol) and 4-methoxyaniline (120 mg, 0.97 mmol) to produce 73 mg of **4d** in 33% yield, faint yellow solid, mp 142~144 ℃; ^{1}H NMR δ ppm 3.02 (3H, s, NCH$_3$), 3.72 (3H, s, OCH$_3$), 6.85 (2H, d, J = 8.8 Hz, ArH-3′, 5′), 7.13 (1H, t, J = 8.0 Hz, ArH-6), 7.35 (1H, d, J = 8.0 Hz, ArH-5), 7.55 (1H, t, J = 8.0 Hz, ArH-7), 7.83 (2H, d, J = 8.8 Hz, ArH-2′, 6′), 7.98 (1H, d, J = 8.0 Hz, ArH-8), 8.07 (1H, br, NH), 8.87 (1H, s, NH); MS m/z (%) 281 (M + 1, 100).

2-(4-Methoxyphenyl)amino-4-(N-morpholino)quinazoline (4e). Starting with 4-(2-chloro-quinazolin-4-yl)morpholine (**3e**) (130 mg, 0.52 mmol) and 4-methoxyaniline (95 mg, 0.77 mmol) to produce 68 mg of **4e** in 39% yield, white solid, mp 141~143 ℃; ^{1}H NMR δ ppm 3.63 (4H, t, J = 4.4 Hz, 2 × CH$_2$), 3.73 (3H, s, OCH$_3$), 3.81 (4H, t, J = 4.4 Hz, 2 × CH$_2$), 6.88 (2H, d, J = 8.8 Hz, ArH-3′, 5′), 7.18 (1H, td, J = 8.0 and 1.2 Hz, ArH-6), 7.49 (1H, dd, J = 8.0 and 1.2 Hz, ArH-5), 7.62 (1H, td, J = 8.0

and 1.2 Hz, ArH-7), 7.78 (2H, d, J = 8.8 Hz, ArH-2′, 6′), 7.78 (1H, d, J = 8.0 Hz, ArH-8), 9.15 (1H, s, NH); MS m/z (%) 337 (M + 1, 100).

4-(*N*-cyclopropyl)amino-2-(4-methoxyphenyl)aminoquinazoline (4f). Starting with 2-chloro-4-(*N*-cyclopropyl)aminoquinazoline (**3f**) (215 mg, 0.98 mmol) and 4-methoxy aniline (184 mg, 1.49 mmol) to produce 103 mg of **4f** in 33% yield, faint yellow solid, mp 192~194 °C; ^{1}H NMR (CDCl$_3$) δ ppm 0.94-0.99 (4H, m, CH$_2$×2), 1.64 (1H, m, CH), 3.82 (3H, s, OCH$_3$), 6.87 (2H, d, J = 8.8 Hz, ArH-3′, 5′), 7.21 (1H, t, J = 8.0 Hz, ArH-6), 7.42 (1H, d, J = 8.0 Hz, ArH-5), 7.56 (1H, t, J = 8.0 Hz, ArH-7), 7.65 (2H, d, J = 8.8 Hz, ArH-2′, 6′), 8.02 (1H, d, J = 8.0 Hz, ArH-8), 10.27 (1H, s, NH), 13.26 (1H, s, NH); MS m/z (%) 307 (M + 1, 100).

Coupling reaction procedure for preparations of 4a, 5, 6, and 7 series. A mixture of a 4-substituted 2-chloroquinazoline (**3**) (1.0 equiv) and a *para*-substituted aniline or *para*-substituted *N*-methylaniline (1.05-1.5 equiv) in EtOH (2.5 mL) in a closed vial was heated under microwave irradiation at 150 ºC for 15–25 min monitored by TLC until the reaction finished. The mixture was poured into water, and pH adjusted to 10 with NaHCO$_3$. The solid crude product was collected, washed, and purified by flash column chromatography (gradient elution: MeOH/CH$_2$Cl$_2$, 0–5%) to give corresponding target compound.

4-(*N*-Cyclopentyl)amino-2-(4-methoxyphenyl)aminoquinazoline (4a). Starting with 2-chloro-4-(*N*-cyclopentyl)aminoquinazoline (**3a**) (340 mg, 1.37 mmol) and 4-methoxyaniline (205 mg, 1.65 mmol) to produce 303 mg of **4a** in 66% yield, faint yellow solid, mp 211~213 °C; ^{1}H NMR δ ppm 1.58 (2H, m, CH$_2$), 1.77 (4H, m, CH$_2$×2), 1.99 (2H, m, CH$_2$), 3.78 (3H, s, OCH$_3$), 4.50 (1H, br, s, CH), 7.01 (2H, d, J = 8.4 Hz, ArH-3′, 5′), 7.44 (1H, t, J = 8.0 Hz, ArH-6), 7.48 (2H, d, J = 8.4 Hz, ArH-2′, 6′), 7.54 (1H, d, J = 8.0 Hz, ArH-5), 7.81(H, t, J = 8.0 Hz, ArH-7), 8.51 (1H, d, J = 8.0 Hz, ArH-8), 9.39 (1H, br, NH), 10.34 (1H, s, NH); MS m/z (%) 335 (M + 1, 100).

4-(*N*-Cyclopentyl)amino-2-(*N*-(4-methoxyphenyl)-*N*-methyl)aminoquinazoline (5a). Starting with **3a** (260 mg, 0.95 mmol) and 4-methoxy-*N*-methylaniline (160 mg, 1.16 mmol) to produce 270 mg of **5a** in 82% yield, white solid, mp 216-218 °C; ^{1}H NMR δ ppm 1.53 (2H, m, CH$_2$), 1.72 (4H, m, CH$_2$ ×2), 1.93 (2H, m, CH$_2$), 3.57 (3H, s, NCH$_3$), 3.82 (3H, s, OCH$_3$), 4.33 (1H, f, J = 7.2 Hz, CH), 7.09 (2H, d, J = 8.4 Hz, ArH-3′, 5′), 7.42 (1H, t, J = 8.0, ArH-6), 7.43 (3H, m, ArH-2′, 6′), 7.78 (2H, m, ArH-5, 7), 8.51 (1H, d, J = 8.0 Hz, ArH-8), 9.36 (1H, br, NH); MS *m/z* (%) 349 (M + 1, 100), 281 (M 67, 70).

4-(3-Hydroxypropyl)amino-2-((*N*-(4-methoxyphenyl)-*N*-methyl)aminoquinazoline (5b). Starting with **3b** (160 mg, 0.67 mmol) and *N*-methyl-4-methoxyaniline (112 mg, 0.81 mmol) to produce 165 mg of **5b** in 73% yield, white solid, mp 188~190 °C; ^{1}H NMR δ ppm 1.75 (2H, m, CH$_2$), 3.35-3.43 (4H, m, CH$_2$×2), 3.56 (3H, s, NCH$_3$), 3.82 (3H, s, OCH$_3$), 4.60 (1H, s, OH), 7.09 (2H, d, J = 8.8 Hz, ArH-3′, 5′), 7.43 (1H, m, ArH-6), 4,45 (2H, d, J = 8.8 Hz, ArH-2′, 6′), 7.76 (2H, m, ArH-5, 7), 8.37 (1H, d, J = 8.0 Hz, ArH-8), 9.79 (1H, br, NH); MS *m/z* (%) 339 (M + 1, 100).

2-(*N*-(4-Methoxyphenyl)-*N*-methyl)amino-4-propylaminoquinazoline (5c). Starting with **3c** (240 mg, 1.08 mmol) and 4-methoxy-*N*-methylaniline (180 mg, 1.31 mmol) to produce 270 mg of **5c** in 86% yield, white solid, mp 191~193 °C; ^{1}H NMR δ ppm 0.84 (3H, t, J = 7.2 Hz, CH$_3$), 1.58 (2H, m, CH$_2$), 3.39 (2H, t, J = 7.2 Hz, NCH$_2$,), 3.57 (3H, s, NCH$_3$), 3.82 (3H, s, OCH$_3$), 7.09 (2H, d, J = 8.8 Hz, ArH-3′, 5′), 7.42 (2H, d, J = 8.8 Hz, ArH-2′, 6′), 7.43 (1H, t, J = 8.0, ArH-6), 7.76 (2H, m, ArH-7,5), 8.40 (1H, d, J = 8.0 Hz, ArH-8), 9.87 (1H, br, NH); MS *m/z* (%) 322 (M + 1, 100).

2-(*N*-(4-Methoxyphenyl)-*N*-methyl)amino-4-methylaminoquinazoline (5d). Starting with **3d** (185 mg, 0.96 mmol) and 4-methoxy-*N*-methylaniline (160 mg, 1.16 mmol) to produce 214 mg of **5d** in 76% yield, white solid, mp 204~206 °C; ^{1}H NMR δ ppm 3.02 (3H, br. s, NCH$_3$) , 3.58 (3H, s, NCH$_3$), 3.83 (3H, s, OCH$_3$), 7.11 (2H, d, J = 8.8 Hz, ArH-3′, 5′), 7.43 (1H, m, ArH-6), 7.44 (2H, d, J = 8.8 Hz,

ArH-2′, 6′), 7.77 (2H, m, ArH-5, 7), 8.37 (1H, d, J = 8.0 Hz, ArH-8), 9.91 (1H, br, NH); MS m/z (%) 295 (M + 1, 100).

2-(*N*-(4-Methoxyphenyl)-*N*-methyl)amino-4-(N-morpholino)quinazoline (5e). Starting with **3e** (124 mg, 0.52 mmol) and 4-methoxy-*N*-methylaniline (75 mg, 0.55 mmol) to produce 138 mg of **5e** in 80% yield, white solid, mp 143-145°C; ^{1}H NMR δ ppm 3.48 (4H, J = 4.2 Hz, NCH$_2$×2), 3.48 (3H, s, NCH$_3$), 3.69 (4H, t, J = 4.2 Hz, OCH$_2$×2), 3.78 (3H, s, OCH$_3$), 6.92 (2H, d, J = 8.8, ArH-3′, 5′), 7.13 (1H, td, J = 8.0 and 1.2 Hz, ArH-6), 7.27 (2H, d, J = 8.8 Hz, ArH-2′, 6′), 7.41 (1H, d, J = 8.0 Hz, ArH-5), 7.57 (1H, td, J = 8.0 and 1.2 Hz, ArH-7), 7.77 (1H, d, J = 8.0 Hz, ArH-8); MS m/z (%) 350 (M + 1, 30), 321 (M − 29, 100).

2-(*N*-(4-Methoxyphenyl)-*N*-methyl)amino-4-(*N*-((tetrahydro-2H-pyran-4-yl)methyl)aminoqui nazoline (5g). Starting with 2-chloro-4-(*N*-((tetrahydro-2H-pyran-4-yl)methyl) aminoquinazolin (**3g**) (138 mg, 0.50 mmol) and 4-methoxy-*N*-methylaniline (75 mg, 0.55 mmol) to produce 153 mg of **5g** in 81% yield, white solid, mp 165-167°C; ^{1}H NMR δ ppm 1.06 (2H, m, CH$_2$), 1.36 (2H, m, CH$_2$), 1.74 (1H, m, CH), 3.07 (2H, t, J = 6.0 Hz, NCH$_2$), 3.15 (2H, t, J = 10.0 Hz, CH$_2$O), 3.44 (3H, s, NCH$_3$), 3.75 (3H, s, OCH$_3$), 3.79 (2H, m, CH$_2$O), 6.92 (2H, d, J = 8.0 Hz, ArH-3′, 5′), 7.07 (1H, td, J = 8.0 and 1.2, ArH-6), 7.25 (2H, d, J = 8.0 Hz, ArH-2′, 6′), 7.31 (1H, d, J = 8.0 Hz, ArH-5), 7.50 (1H, td, J = 8.0 and 1.2 Hz, ArH-7), 7.97 (1H, d, J = 8.0 Hz, ArH-8), 8.03 (1H, t, J = 6.0 Hz, NH); MS m/z 379 (M + 1, 100).

2-(4-Cyanophenyl)amino-4-(*N*-cyclopentyl)aminoquinazoline (6a). Starting with **3a** (249 mg, 1.01 mmol) and 4-cyanoaniline (125 mg, 1.10 mmol) to produce 245 mg of **6a** in 74 % yield, white solid, mp 218~220 °C; ^{1}H NMR δ ppm 1.63 (2H, m, CH$_2$), 1.79 (4H, m, CH$_2$×2), 2.05 (2H, m, CH$_2$), 4.54 (1H, f, J = 7.2 Hz, CH), 7.51 (1H, t, J = 8.0 Hz, ArH-6), 7.59 (1H, d, J = 8.0 Hz, ArH-5), 7.86 (2H, d, J = 8.0 Hz, ArH-2′, 6′), 7.90 (1H, m, ArH-7), 7.91 (3H, d, J = 8.0 Hz, ArH-3′, 5′), 8.55 (1H, d, J = 8.0 Hz, ArH-8), 9.59 and 10.95 (each 1H, s, NH); MS m/z (%) 330 (M + 1, 100).

23

2-(4-Aminophenyl)amino-4-(*N*-cyclopentyl)aminoquinazoline (6b). Starting with **3a** (250 mg, 1.01 mmol) and benzene-1,4-diamine (123 mg, 1.13 mmol) to produce 220 mg of **6b** in 69% yield, yellow solid, mp 223~225 °C; ^{1}H NMR δ ppm 1.57 (2H, m, CH$_2$), 1.72 (4H, m, CH$_2\times2$), 2.00 (2H, m, CH$_2$), 4.51 (1H, br, CH), 6.64 (2H, d, J = 8.4 Hz, ArH-3′, 5′), 7.18 (2H, J = 8.4 Hz, ArH-2′, 6′), 7.40 (1H, t, J = 8.0 Hz, ArH- 6), 7.54 (1H, d, J = 8.0 Hz, ArH-5), 7.77 (1H, t, J = 8.0 Hz, ArH-7), 8.46 (1H, d, J = 8.0 Hz, ArH-8), 9.25 (1H, br, NH), 10.05 (1H, br, NH); MS *m/z* (%) 320 (M + 1, 100), 252 (M − 67, 85).

4-(*N*-Cyclopentyl)amino-2-(4-fluorophenyl)aminoquinazoline (6c). Starting with **3a** (245 mg, 0.99 mmol) and 4-fluoroaniline (140 mg, 1.15 mmol) to produce 315 mg of **6c** in 98% yield, white solid, mp 208~210 °C; ^{1}H NMR δ ppm 1.58 (2H, m, CH$_2$), 1.76 (4H, m, CH$_2\times2$), 1.99 (2H, m, CH$_2$), 4.47 (1H, m, CH), 7.30 (2H, t, $J_{H, F}$ = 8.4 Hz, ArH-3′, 5′), 7.46 (1H, t, J = 8.0 Hz, ArH-6), 7.56 (1H, d, J = 8.0 Hz, ArH-5), 7.62 (2H, dd, $J_{H, F}$ = 8.4 and 4.2 Hz, ArH-2′, 6′), 7.83 (1H, d, J = 8.0 Hz, ArH-7), 8.54 (1H, d, J = 8.0 Hz, ArH-8), 9.48 (1H, s, NH), 10.53 (1H, s, NH); MS *m/z* (%) 323 (M + 1, 100), 255 (M − 67, 97).

4-(*N*-Cyclopentyl)amino-2-(4-hydroxyphenyl)aminoquinazoline (6d). Starting with **3a** (255 mg, 1.03 mmol) and 4-aminophenol (120 mg, 1.10 mmol) to produce 269 mg of **6d** in 83% yield, light yellow solid, mp 169~171 °C; ^{1}H NMR δ ppm 1.57 (2H, m, CH$_2$), 1.73 (4H, m, CH$_2\times2$), 2.00 (2H, m, CH$_2$), 4.50 (1H, br, CH), 6.81 (2H, d, J = 8.0 Hz, ArH-3′, 5′), 7.38 (3H, J = 8.0 z, ArH-2′, 6′ and ArH- 6), 7.51 (1H, d, J = 8.0 Hz, ArH-5), 7.75 (1H, t, J = 8.0 Hz, ArH-7), 8.42 (1H, d, J = 8.0 Hz, ArH-8), 9.06 (1H, br, NH), 9.51 (1H, br, OH), 10.05 (1H, br, NH); MS *m/z* (%) 321 (M + 1, 90), 253 (M − 67, 100).

2-(4-Carboxyphenyl)amino-4-(*N*-cyclopentyl)aminoquinazoline (6e). Starting with **3a** (250 mg, 1.01 mmol) and 4-aminobenzoic acid (151 mg, 1.10 mmol) to produce 240 mg of **6e** in 81% yield, white solid, mp 302~304 °C; ^{1}H NMR δ ppm 1.63 (2H, m, CH$_2$), 1.79 (4H, m, CH$_2\times2$), 2.05 (2H, m,

CH$_2$), 4.57 (1H, f, J = 6.4 Hz, CH), 7.50 (1H, td, J = 8.0 Hz, ArH-6), 7.57 (1H, d, J = 8.0 Hz, ArH-5), 7.79 (2H, d, J = 8.8 Hz, ArH-3′, 5′), 7.86 (1H, t, J = 8.0 Hz, ArH-7), 7.99 (2H, d, J = 8.8 Hz, ArH-2′, 6′), 8.53 (1H, d, J = 8.0 Hz, ArH-8), 9.50 (1H, s, NH), 10.79 (1H, s, NH), 12.90 (1H, s, COOH); MS m/z (%) 349 (M + 1, 100).

2-(4-Cyanophenyl)amino-4-((3-hydroxypropyl)amino)quinazoline (7a). Starting with **3b** (241 mg, 1.01 mmol) and 4-cyanoaniline (125 mg, 1.05 mmol) to produce 48 mg of **7a** in 34 % yield, white solid, mp 177~179 °C; ^{1}H NMR δ ppm 1.84 (2H, f, J = 6.0 Hz, CH$_2$), 3.54 (2H, t, J = 6.0 Hz, NCH$_2$), 3.70 (2H, m, OCH$_2$), 4.62 (1H, br, OH), 7.51 (1H, t, J = 8.0 Hz, H-6), 7.59 (2H, d, J = 8.0 Hz, ArH-5), 7.85 (1H, m, ArH-7), 7.87 (2H, d, J = 8.0 Hz, ArH-2′, 6′), 7.90 (2H, d, J = 8.0 Hz, ArH-3′, 5′), 8.40 (1H, d, J = 8.0 Hz, ArH-8), 10.05 (1H, s, NH), 10.91 (1H, s, NH); MS m/z (%) 320 (M + 1, 100).

2-(4-Aminophenyl)amino-4-((3-hydroxypropyl)aminoquinazoline (7b). Starting with **3b** (240 mg, 1.01 mmol) and benzene-1,4-diamine (120 mg, 1.10 mmol) to produce 196 mg of **7b** in 63% yield, faint yellow, mp 274~276 °C; ^{1}H NMR δ ppm 1.81 (2H, m, CH$_2$), 3.50 (2H, m, CH$_2$), 3.61 (2H, m, CH$_2$), 4.63 (1H, br, OH), 6.63 (2H, d, J = 8.4 Hz, ArH-3′, 5′), 7.18 (2H, br, ArH-2′, 6′), 7.41 (1H, t, J = 8.0 Hz, ArH-6), 7.56 (1H, br. ArH-5), 7.77 (1H, t, J = 8.0 Hz, ArH-7), 8.31 (1H, d, J = 8.0 Hz, ArH-8), 9.58 (1H, br, NH), 10.02 (1H, br, NH); MS m/z (%) 310 (M + 1, 100).

2-(4-Fluorophenyl)amino-4-(3-hydroxypropyl)aminoquinazoline (7c). Starting with **3b** (237 mg, 1.00 mmol) and 4-fluoroaniline (133 mg, 1.05 mmol) to produce 206 mg of **7c** in 66% yield, white solid, mp 185~187 °C; ^{1}H NMR δ ppm 1.80 (2H, f, J = 6.4 Hz, CH$_2$), 3.49 (2H, t, J = 6.4 Hz, CH$_2$), 3.61 (2H, t, J = 6.4 Hz, CH$_2$), 4.65 (1H, br, OH), 7.28 (2H, t, $J_{H,F}$ = 8.4 Hz, ArH-3′, 5′), 7.47 (1H, td, J = 8.0 Hz, ArH-6), 7.57 (1H, d, J = 8.0 Hz, ArH-5), 7.64 (2H, dd, $J_{H,F}$ = 8.4 and 4.2 Hz, ArH-2′, 6′), 7.83 (1H, t, J = 8.0 Hz, ArH-7), 8.36 (1H, d, J = 8.0 Hz, ArH-8), 9.85 (1H, br, NH), 10.42 (1H, br, NH); MS m/z (%) 313 (M + 1, 100).

4-Propylamino-2-(4-fluorophenyl)aminoquinazoline (7d). Starting with **3c** (133 mg, 0.60 mmol) and 4-fluoroaniline (75 mg, 0.67 mmol) to produce 120 mg of **7d** in 67% yield, faint yellow solid, mp 202~204 °C; ^{1}H NMR δ ppm 0.91 (3H, t, J = 7.2 Hz, CH$_3$), 1.65 (2H, six, J = 7.2 Hz, CH$_2$), 3.48 (2H, m, CH$_2$), 7.28 (2H, t, $J_{H,F}$ = 8.4 Hz, ArH-3′, 5′), 7.46 (1H, t, J = 8.0 Hz, ArH-6), 7.56 (1H, d, J = 8.0 Hz, ArH-5), 7.62 (2H, dd, $J_{H,F}$ = 8.4 and 4.2 Hz, ArH-2′, 6′), 7.82 (1H, t, J = 8.0 Hz, ArH-7), 8.39 (1H, d, J = 8.0 Hz, ArH-8), 9.87 (1H, br, NH), 10.44 (1H, br, NH); MS m/z (%) 297 (M + 1, 100).

2-(4-Fluorophenyl)amino-4-(*N*-morpholino)quinazoline (7e). Starting with **3e** (85 mg, 0.34 mmol) and 4-fluoroaniline (45 mg, 0.41 mmol) to produce 86 mg of **7e** in 78% yield, white solid, mp 223~225 °C; ^{1}H NMR δ ppm 3.67 (4H, t, J = 4.2 Hz, 2 × NCH$_2$), 3.81 (4H, t, J = 4.2 Hz, 2 × OCH$_2$), 7.13 (2H, t, $J_{H,F}$ = 8.4 Hz, ArH-3′, 5′), 7.22 (1H, d, J = 8.0 Hz, ArH-6), 7.54 (1H, d, J = 8.0 Hz, ArH-5), 7.64 (1H, dd, J = 8.0 Hz, ArH-7), 7.86 (1H, d, J = 8.0 Hz, ArH-8), 7.91 (2H, dd, $J_{H,F}$ = 8.4 and 4.2 Hz, ArH-2′, 6′), 9.39 (1H, s, NH); MS m/z (%) 325 (M + 1, 100).

2-(4-Aminophenyl)amino-4-(*N*-morpholino)quinazoline (7f). Starting with **3e** (125 mg, 0.50 mmol) and benzene-1,4-diamine (60 mg, 0.57 mmol) to produce 152 mg of **7f** in 94% yield, white solid, mp 195~197 °C; ^{1}H NMR δ ppm 3.59 (4H, t, J = 4.0 Hz, 2 × NCH$_2$), 3.80 (4H, t, J = 4.0 Hz, OCH$_2$ ×2), 4.76 (2H, br, NH$_2$), 6.52 (2H, d, J = 8.0 Hz, ArH-3′, 5′), 7.13 (1H, t, J = 8.4 Hz, ArH-6), 7.42 (1H, d, J = 8.4 Hz, ArH-5), 7.46 (2H, d, J = 8.0 Hz, ArH-2′, 6′), 7.57 (1H, t, J = 8.4 Hz, ArH-7), 7.79 (1H, d, J = 8.4 Hz, ArH-8), 8.83 (1H, s, NH); MS m/z (%) 322 (M + 1, 100).

Mer Tyrosine Kinase assay.[11] Inhibition of Mer kinase by a test compound was measured in the Microfluidic Capillary Electrophoresis (MCE) assay. This activity assay was performed in a 384-well, polypropylene microplate (Greiner BioOne, Monroe, NC) in a final volume of 50 µL in 50 mM Hepes, pH 7.4 containing 0.1% bovine serum albumin (BSA), 0.1% Triton X-100, 10 mM MgCl$_2$ and ATP at 27 µM for the enzyme. All reactions were terminated by addition of 50 µL of 70 mM EDTA.

Phosphorylated and unphosphorylated substrate peptides (EFPIYDFLPAKKK-CONH$_2$ for Mer TK) were separated following a 180 min incubation on a Caliper LabChip EZ Reader II equipped with a 12-sipper chip in separation buffer supplemented with CR-8 and analyzed using EZ Reader software (Caliper Life Sciences; Hopkinton, MA). The assay conditions for MCE assays and screening against 72 kinases are described in Supporting Information (SI).

Antiproliferative activity in cellular assays. According to procedures described previously,[20-22] target compounds were assayed by using the SRB method with a HTCL panel, included human lung carcinoma (A-549), epidermoid carcinoma of the nasopharynx (KB), P-gp-expressing epidermoid carcinoma of the nasopharynx (KBvin), and prostate cancer (DU145). Whereas, MTT method was used to evaluate antitumor activity in human myelogenous leukemia (MV4-11) cell line. The potency of each compound was expressed as GI$_{50}$ value, which represents the molar drug concentration required to cause 50% tumor cell growth inhibition. All data represent at least three independent experiments performed in duplicate.

Aqueous Solubility Determination. Solubility was measured separately at pH 7.4 by using an HPLC-UV method. Test compounds were initially dissolved in DMSO at 10 mg/mL. Ten microliters of this stock solution were spiked into either pH 7.4 phosphate buffer (1.0 mL) with the final DMSO concentration being 1%. The mixture was stirred for 4 h at room temperature, and then concentrated at 10,000 rpm for 5 min. The saturated supernatants were transferred to other vials for analysis by HPLC-UV and detected at 254 nm. Each sample was performed in triplicate. For quantification, a model 1200 HPLC-UV (Agilent) system was used with an Agilent Eclipse XDB-C18 column (150 × 4.6 mm, 5 m) and gradient elution of methanol (MeOH) in water, starting with 60% of MeOH, which was linearly increased up to 80% over 10 min, then slowly increased up to 90% over 15 min. The flow rate was 1.0 mL/min, and injection volume was 15 μL. Aqueous concentration was determined by comparison of the

peak area of the saturated solution with a standard curve plotted as peak area versus known concentrations, which were prepared by solutions of test compound in acetonitrile (ACN) at 50 μg/mL, 25 μg/mL, 12.5 μg/mL, 3.13 μg/mL, 0.78 μg/mL, and 0.20 μg/mL.

Log P Measurement. Using the same DMSO stock solution (10 mg/mL) as above, 10 μL of this solution was added into *n*-octanol (0.6 mL) and water (0.6 mL). The mixture was stirred at room temperature for 24 h and then left to stand overnight. Each solution (ca. 0.2 mL) from two phases was transferred respectively into other vials for HPLC analysis. The instrument and conditions were the same as those for solubility determination. Log P value was calculated by the peak area ratios in n-octane and in water (log $P = \log (S_{oct}/S_{water})$.

Molecular Modeling. All molecular modeling studies were performed with Discovery Studio 3.0 (Accelrys, San Diego, USA). The crystal structure of Mer kinase in complex with UNC569 (PDB code: 3TCP) was downloaded from the RCSB Protein Data Bank (http://www.rcsb.org/pdb) for use in the modeling study. Flexible Docking was used to evaluate and predict in silico binding free energy of the inhibitors and for automated docking. The protein protocol was prepared by several operations, including standardization of atom names, insertion of missing atoms in residues and removal of alternate conformations, insertion of missing loop regions based on SEQRES data, optimization of short and medium size loop regions with the Looper algorithm, minimization of remaining loop regions, calculation of pK, and protonation of the structure. The protein model was typed with the CHARMM force field. A binding sphere with a radius of 8.0 Å was defined through the original ligand (UNC569) as the binding site for the study. The docking protocol employed total ligand and the side chain of amino acids Leu671, Pro672, Phe673, Met674, Asp678, Arg727 and Asn728 flexibility, and the final ligand conformations were determined by the simulated annealing molecular dynamics search method set to a variable number of trial runs. Docked ligand **4b** was further refined using in situ ligand minimization

with the Smart Minimizer algorithm by standard parameters. The implicit solvent model of Generalized Born with Molecular Volume (GBMV) was also used to calculate the binding energies.

Acknowledgements

References.

1   Linger, R. M. A.; DeRyckere, D.; Brandao, L.; Sawczyn, K. K.; Jacobsen, K. M.; Liang, X.; Keating, A. K.; Graham, D. K. *Blood*, **2009**, 114, 2678-2687.

2   O'Leary, M.; Krailo, M.; Anderson, J. R.; Reaman, G. H. *Seminars in Oncology*, **2008**, 35, 484–493.

3   Salzer, W. L.; Devidas, M.; Carroll, W. L.; Winick, N.; Pullen, J.; Hunger, S. P.; Camitta, B.A. *Leukemia*, **2009**, 24, 355–370.

4   Schultz, K. R.; Bowman, W. P.; Aledo, A.; Slayton, W. B.; Sather, H.; Devidas, M.; Wang, C.; Davies, S. M.; Gaynon, P. S.; Trigg, M.; Rutledge, R.; Burden, L.; Jorstad, D.; Carroll, A.; Heerema, N. A.; Winick, N.; Borowitz, M. J.; Hunger, S. P.; Carroll, W. L.; Camitta, B. *Journal of Clinical Oncology*, **2009** 27, 5175–5181.

5   Guttridge, K. L.; Luft, J. C.; Dawson, T. L. *J. Biol. Chem*. **2002**, 277(27), 24057-24066

6   Graham, D. K.; Salzberg, D. B.; Kurtzberg, J.; Sather, S.; Matsushima, G. K.; Keating, A. K.; Liang,

X.; Lovell, M. A.; Williams, S. A.; Dawson, T. L.; Schell, M. J.; Anwar, A. A.; Snodgrass, H. R.; Earp, H. S. *Clin Cancer Res* **2006**, *12*, 2662-2669.

7   Keating, A. K.; Salzberg, D. B.; Sather, S.; Liang, X.; Nickoloff, S.; Anwar, A.; Deryckere, D.; Hill, K.; Joung, D.; Sawczyn, K. K.; Park, J.; Curran-Everett, D.; McGavran, L.; Meltesen, L.; Gore, L.; Johnson, G. L.; Graham, D. K. *Oncogene* **2006**, 25, 6092-6100

8   Linger, R. M. A.; Keating, A. K.; Earp, H. S.; Graham, D. K. *Advances in Cancer Research*, **2008**, 35-83

9   Linger, R. M. A.; Keating, A. K.; Earp, H. S.; Graham, D. K. *Expert Opin. Ther. Tatgets*. **2010**, *14(10)*, 1073-1990.

10   Huang, X.; Finerty, P. Jr.; Walker, J. R.; Butler-Cole, C.; Vedadi, M.; Schapira, M.; Parker, S. A.; Turk, B. E.; Thompson, D. A.; DhePaganon, S. *J. Struct. Biol.* **2009**, *165*, 88-96.

11   Liu, J.; Yang, C.; Simpson, C.; DeRyckere, D.; Deusen, A. V.; Miley, M. J.; Kireev, D.; Norris-Drouin, J.; Sather, S.; Hunter, D.; Korboukh, V. K.; Patel, H. S.; Janzen, W. B.; Machius, M.; Johnson, G. L.; Earp, H. S.; Graham, D. K.; Frye, S. V.; Wang, X. *ACS Med. Chem. Lett.* **2012**, *3*, 129-134.

12   Zhang, W.; Zhang, D.; Stashko, M. A.; DeRyckere, D.; Hunter, D.; Kireev, D.; Miley, M. J.; Cummings, C.; Lee, M.; Norris-Drouin, J.; Stewart, W. M.; Sather, S.; Zhou Y.; Kirkpatrick, G.; Machius, M.; Janzen, W. P.; Earp, H. S.; Graham, D. K.; Frye, S. V.; Wang, X. *J. Med. Chem*. **2013**, *56*, 9683-9692.

13   Zhang, W.; McIver, A. L.; Stashko, M. A.; DeRyckere, D.; Branchford, B. R.; Hunter, D.; Kireev, D.; Miley, M. J.; Norris-Drouin, J.; Stewart, W. M.; Lee, M.; Sather, S.; Zhou Y.; Di Paola, J. A.; Machius, M.; Janzen, W. P.; Earp, H. S.; Graham, D. K.; Frye, S. V.; Wang, X. *J. Med. Chem.* **2013**, 56, 9693-9700.

14 Wang, X. F.; Tian, X. T.; Ohkoshi, E.; Qin, B.; Liu, Y. N.; Wu, P. C.; Hung, H. Y.; Hour, M. J.; Qian, K.; Huang, R.; Bastow, K. F.; Janzen, W. P.; Jin, J.; Morris-Natschke, S. L.; Lee, K. H.; Xie, L. *Bioorg. Med. Chem. Lett*. **2012**, *22*, 6224-6228.

15 Wang, X. F.; Wang, S. B.; Ohkoshi, E.; Wang, L. T.; Hamel, E.; Qian, K.; Morris-Natschke, S. L.; Lee, K. H.; Xie, L. *Eur. J. Med. Chem.* **2013**, *67*, 196-207.

16 Wang, X. F.; Guan, F.; Ohkoshi, E.; Guo, W.; Wang, L.; Zhu, D. Q.; Wang, S. B.; Wang, L. T.; Hamel, E.; Yang, D.; Li, L.; Qian, K.; Morris-Natschke, S. L.; Yuan, S.; Lee, K. H.; Xie, L. *J. Med. Chem*. **2014**, *57*, 1390-1402.

17 Wang, S. B.; Wang, X. F.; Qin, B.; Ohkoshi. E.; Hsieh, K. Y.; Hamel, E.; Cui, M. T.; Zhu, D. Q.; Goto, M.; Morris-Natschke, S. L.; Lee, K. H.; Xie, L. *Bioorg. Med. Chem*. **2015**, *23*, 5740-5747.

18 Smits, R. A.; de Esch, I. J. P.; Zuiderveld, O. P.; Broeker, J.; Sansuk, K.; Guaita, E.; Coruzzi, G.; Adami, M.; Haaksma, E.; Leurs, R.; *J. Med. Chem*. **2008**, *51*, 7855-7865.

19 Sun, L. Q.; Zhu, L.; Qian, K.; Qin, B.; Huang, L.; Chen, C. H.; Lee, K. H.; Xie, L. *J. Med. Chem*. **2012**, *55*, 7219-7229.

20 Boyd, M. R. Status of the NCI preclinical antitumor drug discovery screen, in: *Cancer: Principles and Practice of Oncology Updates*, Devita V. T., Hellman S., Rosenberg S. A. (eds), Lippincott: Philadelphia, **1989**, pp. 1-12.

21 Monks, A.; Scudiero, D.; Skehan, P.; Shoemaker, R.; Paull, K.; Vistica, D.; Hose, C.; Langley, J.; Cronise, P.; Vaigro-Wolff, A.; Gray-Goodrich, M.; Campbell, H.; Mayo, J.; Boyd, M. *J. Natl. Cancer Inst.* **1991**, *83*, 757-766.

22 Houghton P.; Fang, R.; Techatanawat, I.; Steventon, G.; Hylands, P. J.; Lee, C. C. *Methods* **2007**, *42*, 377-387.